Journal of Anatomy

J. Anat. (2013) **223**, pp46–60 doi: 10.1111/joa.12059

The morphology of the mouse masticatory musculature

Hester Baverstock,[1] Nathan S. Jeffery[2] and Samuel N. Cobb[1]

[1]*Centre for Anatomical and Human Sciences, Hull York Medical School, University of Hull, Hull, UK*
[2]*Department of Musculoskeletal Biology, Institute of Ageing and Chronic Disease, University of Liverpool, Liverpool, UK*

Abstract

The mouse has been the dominant model organism in studies on the development, genetics and evolution of the mammalian skull and associated soft-tissue for decades. There is the potential to take advantage of this well studied model and the range of mutant, knockin and knockout organisms with diverse craniofacial phenotypes to investigate the functional significance of variation and the role of mechanical forces on the development of the integrated craniofacial skeleton and musculature by using computational mechanical modelling methods (e.g. finite element and multibody dynamic modelling). Currently, there are no detailed published data of the mouse masticatory musculature available. Here, using a combination of micro-dissection and non-invasive segmentation of iodine-enhanced micro-computed tomography, we document the anatomy, architecture and proportions of the mouse masticatory muscles. We report on the superficial masseter (muscle, tendon and *pars reflecta*), deep masseter, zygomaticomandibularis (anterior, posterior, infraorbital and tendinous parts), temporalis (lateral and medial parts), external and internal pterygoid muscles. Additionally, we report a lateral expansion of the attachment of the temporalis onto the zygomatic arch, which may play a role in stabilising this bone during downwards loading. The data presented in this paper now provide a detailed reference for phenotypic comparison in mouse models and allow the mouse to be used as a model organism in biomechanical and functional modelling and simulation studies of the craniofacial skeleton and particularly the masticatory system.

Key words: contrast-enhanced; jaw closing muscles; masseter; micro-computed tomography; murine; *Mus musculus*; muscular anatomy; pterygoid; temporalis.

Introduction

The mouse (*Mus musculus*) has dominated work on the development, genetics and evolution of the mammalian skull and associated soft-tissue for decades. During this time the emphasis has shifted from one of general qualitative description of changes at the cellular level, and to a lesser extent at the organ system level, to the quantification and investigation of morphological outcomes following genetic and/or experimental manipulation, from dietary regimes through to surgical interventions (Maedaa et al. 1987; Byron et al. 2004; Yamada et al. 2006; Kyrkanides et al. 2007; Byron et al. 2008). As detailed knowledge of mouse craniofacial anatomy is a prerequisite to such work it is generally assumed that this essential knowledge base is well established. Authors have focused attention on the anatomy of the brain (Klintworth, 1968), limbs (Pomikal & Streicher, 2010), internal organs (Berry, 1900; Roberts, 1975) and the embryology (Kaufman, 1992; Brune et al. 1999; Kaufman & Bard, 1999) of the mouse, with very few detailed descriptions of mouse musculature or craniofacial skeletal anatomy, and no accurate description of the masticatory musculature of this species is available in the literature.

Although mouse models have been widely used in many scientific disciplines for decades there has been a recent resurgence in the use of mice to explore morphological questions, and this species is proving extremely valuable in understanding craniofacial development, morphology, function and evolution. Several authors have employed the mouse in studies of craniofacial morphological development and variation (Leamy, 1993; Christian Peter, 2002; Byron et al. 2004; Morriss-Kay & Wilkie, 2005; Willmore et al. 2006a; Vecchione et al. 2007; Boughner et al. 2008; Hallgrimsson & Lieberman, 2008; Lieberman et al. 2008; Cray et al. 2011). Contemporary investigation of integration and modularity has also often focused on the mouse as a model (Mezey et al. 2000; Klingenberg et al. 2003; Hallgrímsson et al. 2004a,b, 2006) and this species has

Correspondence
Hester Baverstock, Centre for Anatomical and Human Sciences, Hull York Medical School, University of Hull, Hull HU6 7RX, UK.
E: hester.baverstock@hyms.ac.uk

Accepted for publication *11 April 2013*
Article published online *20 May 2013*

played a significant role in the understanding of the adaptive evolution of morphology and the function of genetics in such evolution (Atchley et al. 1985a,b, 1988; Cheverud et al. 1991; Klingenberg & Leamy, 2001; Willmore et al. 2006b; Ravosa et al. 2008; Renaud et al. 2010). Additionally, medical and dental science has benefitted from the mouse as a model through the investigation of pathological conditions affecting craniofacial morphology: *Cleft lip* (Chai & Maxson, 2006; Parsons et al. 2008); *Down Syndrome* (Richtsmeier et al. 2002; Hill et al. 2007); *Craniosyntosis* (Perlyn et al. 2006); *Midfacial retrusion* (Lozanoff et al. 1994); *Craniofacial dysmorphology* (Tobin et al. 2008). As the mouse has in the past, and continues to play, such a crucial role in the advancement of understanding of craniofacial development, morphology and evolution it is surprising that very little published data exists regarding the anatomy, and in particular the muscular anatomy of the craniofacial complex of *Mus musculus.*

Despite the paucity of published descriptive mouse anatomy, a significant amount of literature exists regarding rodent masticatory anatomy in general (Greene, 1936; Yoshikawa & Suzuki, 1969; Turnbull, 1970; Hiiemae & Houston, 1971; Weijs, 1973; Weijs & Dantuma, 1975; Coldiron, 1977; Woods & Howland, 1979; Janis, 1983; Woods & Hermanson, 1985; Offermans & De Vree, 1989; Ball & Roth, 1995; Satoh, 1997; Olivares et al. 2004; Satoh & Iwaku, 2004, 2006; Hautier & Saksiri, 2009; Satoh & Iwaku, 2009; Druzinsky, 2010a,b; Cox & Jeffery, 2011) as well as bite force and feeding mechanics in rodents (Hiiemäe & Ardran, 1968; Gorniak, 1977; Robins, 1977; Mosley & Lanyon, 1998; Satoh, 1998, 1999; Nies & Young Ro, 2004; Freeman & Lemen, 2008a,b; Williams et al. 2009). Patel (1978) presented a paper regarding the bone–muscle complex of the masticatory apparatus of *Mus musculus*. This study, however, was investigated through dissection alone and, given the size of the mouse, it is appreciably incomplete and provides little detail of the origins and insertions of the muscles. To the best of the authors' knowledge no other literature exists regarding either the muscular anatomy or the bite force and feeding mechanics of *Mus musculus*.

In this study we present, for the first time, a detailed description of the masticatory apparatus of *Mus musculus.* Using contemporary high resolution micro-computed tomography (micro-CT) with iodine staining, complemented by more traditional dissection techniques we provide a comprehensive description of mouse masticatory musculature that will enable this model organism to be utilised further in an array of disciplines and fields. The methodology of using contrast-enhanced micro-CT imaging coupled with reconstruction techniques is the same as that used by Cox & Jeffery (2011), based upon the work of Metscher (2009) and Jeffery et al. (2011). While micro-CT imaging methods have been employed in quantitative studies of variation (Hallgrímsson et al. 2007) and development (Parsons et al. 2008) in the craniofacial region of mice, the use of contrast-enhanced micro-CT imaging to document non-invasively and to incorporate muscular architecture in such studies thus far remains a little utilised technique. Such contrast-enhanced scanning techniques are more commonly utilised in vascular and cardiac research, both in humans (Aslanidi et al. 2012) and other mammals including mice (Badea et al. 2008), and even to image anthropod circulatory systems (Wirkner & Richter, 2004; Wirkner & Prendini, 2007). These techniques have also been used to investigate jaw muscle anatomy in the alligator (Tsai & Holliday, 2011). The reporting of accurate three-dimensional reconstructions of mammalian post-natal craniofacial musculature from contrast-enhanced micro-CT imaging to provide valuable detail for comparative, developmental, functional and quantitative studies of morphology is, however, so far limited to the rat, squirrel, guinea pig and spiny rat (Cox & Jeffery, 2011; Cox et al. 2012; Hautier et al. 2012). The present study sits alongside the work of Cox & Jeffery (2011) in providing a direct comparison with those three rodents that have been described using the same technique as presented here.

The ongoing status of the mouse as an ideal model organism for investigation and understanding craniofacial development, morphology, function and evolution, combined with exciting and fast-moving developments in the field of comparative anatomy and morphology, has resulted in the urgent need for an excellent description of mouse masticatory anatomy.

This study constructs the foundation for a series of future investigations of form and function. Many authors have taken advantage of the versatility of the mouse in the investigation of variance, canalisation, modularity, integration, functional significance and other fundamental areas of focus in the exploration of form, function and evolution. This large body of studies has included comparative work of different strains, species (Auffray et al. 1996; Cordeiro-Estrela et al. 2006; Macholán, 2008; Macholán et al. 2008), geographic populations (Corti & Rohlf, 2001; Renaud & Michaux, 2007; Macholán et al. 2008), hybrids (Debat et al. 2006) and mutant (Hallgrímsson et al. 2006; Perlyn et al. 2006; Kawakami & Yamamura, 2008) mice. The present study is limited to one species but the detailed and precise anatomical investigation of *Mus musculus* provided here will be utilised in future investigations characterising functionally significant variations in morphology among both different mutant strains and rodent species. Not only will this current work allow the investigation of the functional significance of variation and the role of mechanical forces in the development of the craniomaxillary complex through computational mechanical modelling techniques such as finite element analysis (FEA) and multibody dynamic modelling (MDA), it will also serve as an invaluable reference for phenotypic comparison with other strains and species of mice.

Materials and methods

Dissection

Detailed dissection was carried out on four *Mus musculus* specimens. These specimens were acquired from Newton Resources (Jarrow, UK). Using a micro-dissection kit each specimen was carefully dissected to reveal muscle insertions, attachments and morphology. Superficial muscles were first retracted to reveal deep muscles, and later removed. Individual muscle masses from one specimen of *Mus musculus* were then collected using digital scales. The dissection was documented and photographed using a Canon G9 digital camera (Fig. 2).

Three-dimenstional (3D) skull and muscle reconstruction

Contrast-enhanced micro-CT data for one adult specimen of *Mus musculus* (adult, BALB/c background strain) was carried out by one of us (N.S.J.; see Jeffery et al. 2011). This specimen was acquired post-mortem from Charles River UK Ltd.

A solution of iodine potassium iodide (I2KI) was used as the contrast agent to increase the differential attenuation of X-rays among the soft tissues. This technique has been shown not only to differentiate effectively between individual muscles and bone, but also to demonstrate patterns of muscle fibres and fascicles alongside connective tissues (Cox & Jeffery, 2011; Jeffery et al. 2011).

The specimen was fixed in a phosphate-buffered formal saline solution (polymerized formaldehyde dissolved as a 4% solution in phosphate-buffered saline, allowing for the long-term storage with limited tissue shrinkage) and then placed in 3.75% I2KI contrast agent for 7 days. Although it is possible that muscle shrinkage may occur with this technique, the effect is likely to be relatively small given the low concentration of I2KI used and should be consistent across all muscles, and thus should have no effect on the relative proportions reported or qualitative muscle descriptions. The specimen was then imaged with the Metris X-Tek custom 320 kV bay system at the EPSRC-funded Henry Moseley X-ray Imaging Facility at the University of Manchester. Imaging parameters were optimised for the individual specimen to maximise the spatial and contrast resolution (75 kV; 105 uA). Voxel resolution was isotropic with vertices of 0.033 mm (Jeffery et al. 2011).

The contrast-enhanced micro-CT images were viewed using AVISO6.3, 3D visualisation software designed for visualisation, analysis and modelling of scientific data (Aviso6, Visualisation Sciences Group, Berlin, Germany).

A three-dimensional reconstruction of the masticatory musculature of *Mus musculus* was carried out using the segmentation function of AVISO6.3.

Each masticatory muscle, major masticatory tendon and the craniofacial skeleton and mandible were individually reconstructed. The techniques of contrast enhancement of muscles prior to scanning results in clarity and distinction of individual muscles but has the disadvantage of reducing the contrast difference between muscle and bone. As iodine as a contrast agent reduces the contrast resolution between bone and the surrounding tissues, a scan is produced in which greyscale values are not sufficiently different between muscles and bone, and thus the automated division of these two different materials that is usually possible with a CT scan (through use of a threshold function available in visualisation software such as AVISO6.3) is not possible here. Consequently, all muscle and bone reconstructions were built manually. The contrast-enhanced micro-CT scan was loaded into AVISO6.3, and muscles of interest were carefully identified and painted. Where appropriate, an interpolation function was used to insert material between two selected areas approximately 10 slices apart to improve the efficiency of the process. A smoothing function was applied to reduce the blocky appearance of the reconstruction.

Attachment areas of the muscles were established through segmentation of the contrast-enhanced micro-CT scan independent of that of the muscle volumes. While muscle boundaries on the scan are distinguished via the appearance of a darker greyscale band between the muscle in question and adjacent structures, attachment areas were determined as regions of the scan in which no darker band was present between muscle and bone, and instead, a merging of the greyscale appearance of the two was observable. The authors acknowledge that the subjective nature of this method may introduce some error.

Following completion of the 3D reconstruction, an output of each individual muscle volume was calculated by AVISO6.3. Assuming a muscle density of 1.0564 g cm^{-3}, individual muscle masses were calculated (mass = volume $\times$ density) (Murphy & Beardsly, 1974). Volumes, masses and percentages of muscles are outlined in Table 1.

The masticatory musculature revealed through both dissection and 3D muscle reconstructions was compared to that in previous literature. The literature consulted was as follows: Ball & Roth, 1995 (*Sciurus, Microsciurus, Sciurillus, Tamiasciurus, Tamias, Glaucomys*); Byrd, 1981 (*Cavia*); Cox, 2011 (*Sciurus, Cavia, Rattus*); Druzinsky, 2010a (*Aplondontia, Cynomys, Tamias, Marmota, Ratufa, Sciurus, Thomomys*); Gorniak, 1977 (Mesocricetus); Greene, 1935 (*Rattus*); Hautier & Saksiri, 2009; (*Laonastes*); Hautier, 2010 (*Ctenodactylus*); Offermans & De Vree, 1989 (*Pedetes*); Olivares et al. 2004 (*Aconaemys, Octomys, Tympanoctomys, Spalacopus, Octodon, Octodontomys*); Rinker, 1954 (*Sigmodon, Oryzomys, Neotoma, Peromyscus*); Rinker & Hooper, 1950 (*Reithrodontomys*); Satoh, 1997, 1998, 1999 (*Apodemus, Clethrionomys*); Satoh & Iwaku, 2004 (*Mesocricetus, Cricetulus, Tscherkia, Phodopus*); Satoh & Iwaku, 2006 (*Onychomys*); Satoh & Iwaku, 2009 (*Neotoma, Peromyscus*); Turnbull, 1970 (*Scuirus, Rattus, Hystrix*); Weijs, 1973 (*Rattus*); Wood, 1965 (*Marmota, Myocastor, Ondatra*); Woods, 1972 (*Proechimys, Echimys, Isothrix, Mesomys, Myocastor, Octodon, Ctenomys, Erethizon, Cavia, Chinchilla, Dasyprocta, Thryonomys, Petromus*); Woods & Howland, 1979 (*Capromys, Geocapromys, Plagiodontia, Myocastor*); Woods & Hermanson, 1985 (*Capromys, Geocapromys, Plagiodontia, Myocastor, Echimys, Octodon, Erethizon, Coendou, Dasyprocta, Atherurus, Thryonomys, Petromus*).

Nomenclature

Despite there being very little published work regarding the craniofacial anatomy and musculature in *Mus musculus*, a number of publications exist detailing the masticatory anatomy of species in the rodent order, including the rat (Greene, 1936; Hiiemae & Houston, 1971; Weijs, 1973; Cox & Jeffery, 2011); capromyid rodents (Woods & Howland, 1979); hystricognath rodents (Woods & Hermanson, 1985); new world squirrels (Ball & Roth, 1995); old world hamsters (Satoh & Iwaku, 2004); northern grasshopper mouse (Satoh & Iwaku, 2006); Loatian rock rat (Hautier & Saksiri, 2009); mountain beaver (Druzinsky, 2010a,b) and many more. A

Table 1 Volumes, masses and percentages of the masticatory muscles of *Mus musculus.*

	Muscles volumes estimated from dissection, mm^3	Muscle volumes outputted from segmentation, mm^3	Muscle masses calculated from segmentation, g	Percentage of overall muscle mass or volume, %	Percentage volume of composite parts to individual muscle, %
Superficial masseter (total)	64	58.50	0.062	19.13	
Muscle		52.83	0.056		91.82
Tendon		4.71	0.005		8.18
Pars reflecta		0.96	0.001		1.67
Deep masseter (total)	100	101.89	0.108	33.32	
Zygomaticomandibularis (total)	25	26.92	0.028	8.08	
Anterior		15.71	0.017		58.38
Posterior		3.52	0.004		13.07
Infraorbital		7.17	0.008		26.63
Tendon		0.52	0.001		1.92
Temporalis (total)	60	68.63	0.073	22.44	
Lateral		15.98	0.017		23.28
Medial		52.65	0.056		76.72
Pterygoid (total)	42	49.87	0.053	16.31	
External	10	14.49	0.015	4.74	29.06
Internal	32	35.38	0.037	11.56	70.94

number of different nomenclatures currently exist throughout this body of literature as regards both rodent and general mammalian craniofacial muscular anatomy (Druzinsky et al. 2011). In this paper we will follow the system of a number of authors, with three layers of the masseter observed and identified as the superficial masseter, the deep masseter, and the zygomaticomandibularis. The temporalis is also divided into two parts, the lateral and medial temporalis, reflecting their anatomical relationship. The pterygoids are referred to in reference to their origin on and in the pterygoid fossa, as the internal and external pterygoid muscles (Turnbull, 1970; Weijs, 1973; Ball & Roth, 1995; Cox & Jeffery, 2011).

Other authors have opted for different nomenclatures: some authors have named the three layers of the masseter as the superficial, lateral and medial masseter (Wood, 1965; Woods, 1972; Hautier & Saksiri, 2009); others use a combination of the latter system and that used in this paper (Offermans & De Vree, 1989; Satoh & Iwaku, 2004, 2006, 2009; Druzinsky, 2010a,b). An additional variation found is in the naming of the rostral expansion of the innermost layer of the masseter, referred to here as the infraorbital zygomaticomandibular, sometimes referred to as the maxillomandibularis (Coldiron, 1977; Janis, 1983).

The sole published work specifically regarding the anatomy of the masticatory muscles of *Mus musculus* (Patel, 1978) combines a number of the nomenclatures described above. Patel (1978) differentiates and classifies the masticatory muscles of the mouse as the superficial masseter, deep masseter (consisting of an anterior deep masseter, infraorbital part of the anterior deep masseter, and posterior deep masseter), temporalis (anterior fasciculus, posterior fasciculus and zygomaticus fasciculus) and the pterygoids (external and internal).

The nomenclature elected in this paper has been chosen for its consistency with that used in the literature for most other mammalian groups (Storch, 1968; Coldiron, 1977; Janis, 1983; Druzinsky et al. 2011) and for its uniformity with Cox & Jeffery (2011) who have applied the same techniques reported here to other rodent taxa. This system is also favoured as it clearly reflects the anatomical relationships and positions of the musculature.

Results

Figure 1 illustrates the bony anatomy of the cranium and mandible of *Mus musculus.* Enhanced photographic images of dissection results are given in Fig. 2. Figures 3–6 show the enhanced micro-CT 3D reconstructions of the muscles of mastication in *Mus musculus.* Table 1 gives the corresponding muscle volumes, masses and percentages.

Superficial masseter

The superficial masseter muscle is clearly distinguished both on micro-CT and through dissection. A significant unipenate masticatory muscle, the superficial masseter and its tendon account for 19% of the total muscle mass (Table 1).

Alongside its tendinous sheet that covers about one-third of the lateral surface, the superficial masseter runs obliquely from the anterior portion of the cranium to the posterior portion of the mandible. Roughly triangular in shape and passing obliquely, this muscle directly overlies approximately half of the deep masseter, which lies immediately medial to the superficial muscle (Figs 2A and 3).

The tendinous origin of the superficial masseter attaches to a small process on the maxillary bone of the cranium, immediately medioventral to the infraorbital foramen. Fibres originating from the tendinous sheet run posteriorly, following the oblique path of the tendon and muscle, and insert onto the body of the mandible on both the lateral and medial surfaces (Fig. 6A).

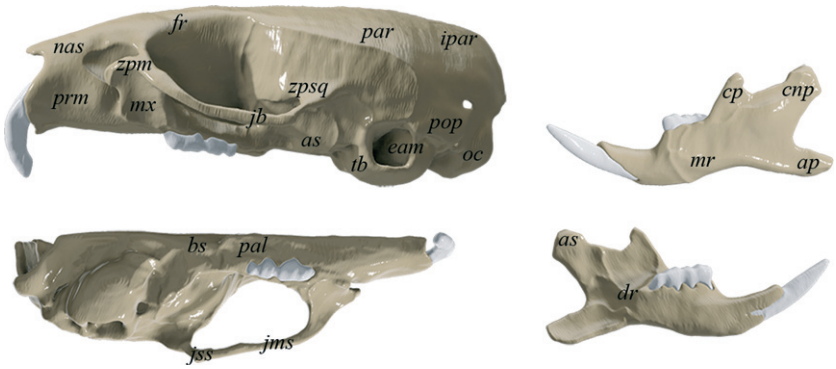

Fig. 1 Key anatomical regions on the cranium and mandible in *Mus musculus*: as, articular surface; cnp, condyloid process; ap, angular process; mr, masseteric ridge; cp, coronoid process; dr, dental ridge; prm, premaxilla; nas, nasal; fr, frontal; aef, anterior ethmoidal foramen; mx, maxilla; zpm, zygomatic process of maxilla; bs, basosphenoid; par, parietal; zpsq, zygomatic process of squamosal bone; ipar, interparietal; eam, external auditory meatus; tb, tympanic bulla; pop, paraoccipital process; oc, occipital condyle; pal, palatine; as, alisphenoid; jb, jugal bone; jss, jugosquamosal suture; jms, jugomaxillary suture.

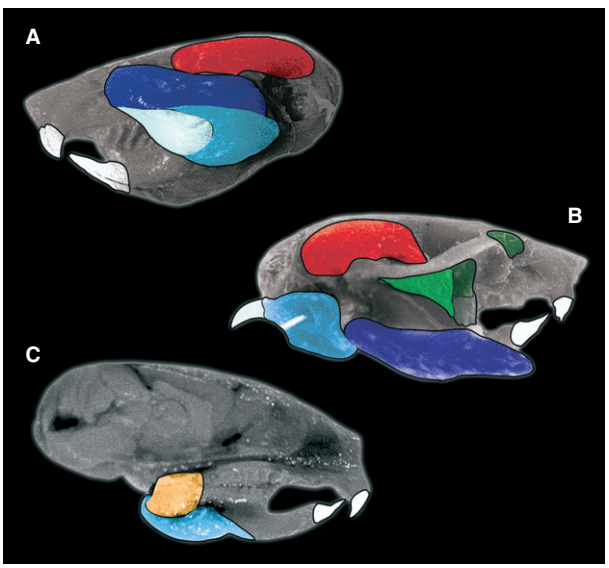

Fig. 2 Graphically enhanced photographs of *Mus musculus* dissection, highlighting major masticatory muscles. (A) Lateral view with skin removed to reveal the temporalis, deep masseter and superficial master muscles. (B) Lateral view with skin removed and both superficial and deep masseter muscles retracted to reveal the zygomaticomandibularis muscle with its infraorbital and anterior regions alongside its tendon. (C) Bisected sagittally to reveal the medial surface of the mandible, with the internal pterygoid and the reflected portion of the superficial masseter. Colour key corresponds to that of Fig. 3.

The superficial masseter has a slender yet lengthy insertion along the ventral border of the mandible. This attachment area lays on both the ventromedial and the ventrolateral surfaces. On the lateral surface, directly beneath the attachment of the deep masseter, this attachment runs from the angle of the mandible to a position ventral to the first molar (Fig. 4E). Similarly, on the medial surface, reflected fibres run from the angle of the mandible to a position ventral to the first molar, with the height of the attachment area increasing in the portion beneath the third molar (Fig. 4F).

A dorsal elongation of the reflected part of the superficial masseter onto the medial surface of the mandible is present. This pars reflecta (Turnbull, 1970; Woods, 1972; Weijs, 1973; Cox & Jeffery, 2011; Druzinsky et al. 2011) attaches along a clearly defined ridge just anterior to the attachment of the internal pterygoid (Figs 3 and 4F).

Deep masseter

The deep masseter is the largest masticatory muscle in the mouse, accounting for 33% of the overall muscle mass (Table 1). This large muscle lying medial to the superficial masseter takes the form of a broad parallelogram, spanning the length of the jugal bone and covering the majority of the mandible (Fig. 3).

Whereas in other rodents a clear division of the deep masseter into anterior and posterior parts is reported (Cox & Jeffery, 2011), in the mouse no clear distinction between two such regions was found on either dissection or segmentation of micro-CT images. A number of septa within the deep masseter are visible on micro-CT, yet none of these is fully discernible as an anterior–posterior divide and no variation in fibre direction suggestive of such a separation was observed (Fig. 6). The deep masseter is thus reported as a single muscle in the present study.

The deep masseter originates from the ventrolateral surface of the jugal bone. This attachment spans almost the entire length of this bone, running anteriorly from the anterior-most point on the rim of the zygomatic process of the maxilla, to the jugosquamosal suture (Fig. 4). Muscle fibres run posteroventrally from their origin on the jugal bone to meet their attachment area on the surface of the mandible (Fig. 6).

The deep masseter inserts onto the lateral surface of the mandible with an attachment area so great that it

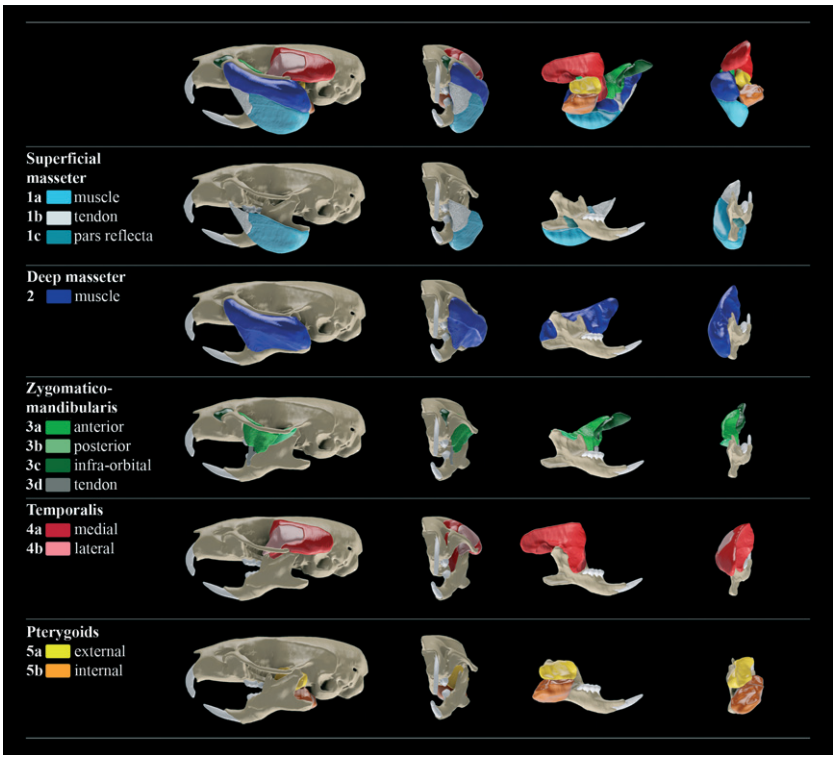

Fig. 3 Three-dimensional reconstruction of masticatory apparatus, with insets showing individual muscles on the cranium and mandible.

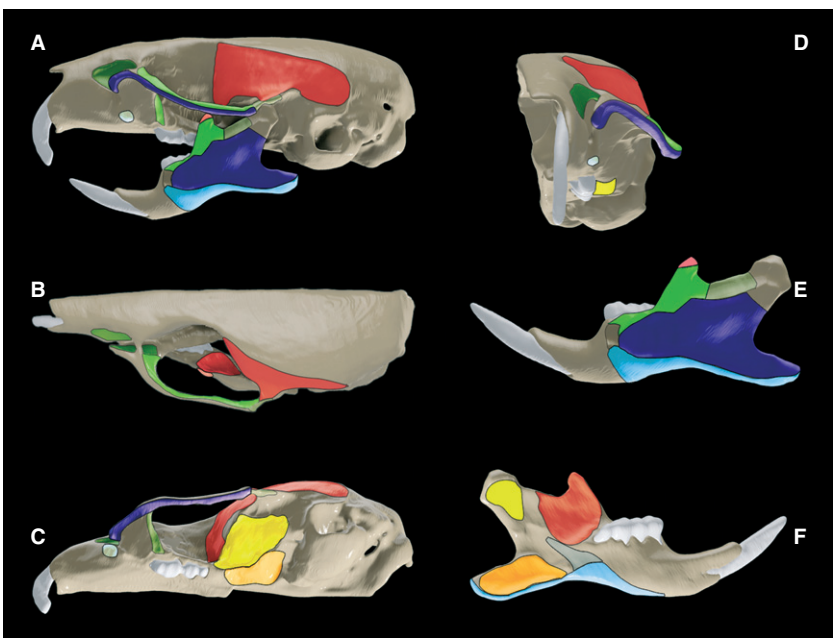

Fig. 4 Masticatory muscle attachment areas. See Fig. 3 for colour key.

covers a large proportion of this surface. This attachment sits directly above that of the superficial masseter and below that of the anterior and posterior zygomaticomandibular, stretching across the surface of the mandible from the angle to a point ventral to the first molar. The inferior border of this attachment runs from the angular process, along the masseteric ridge, to a point ventral to the anterior border of M1. The anterior border of this attachment begins at the point of greatest curvature between the angular process and the condylar process,

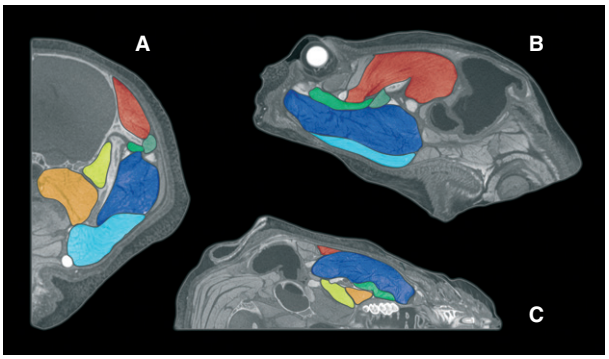

Fig. 5 Contrast-enhanced micro-CT slices, graphically enhanced to visualise masticatory muscles: (A) coronal section; (B) sagittal section; (C) transverse section. See Fig. 3 for colour key.

runs anterodorsally to meet the inferior border of the attachment of the posterior zygomaticomandibularis, and then passes posteroventrally to the anterior-most point on the masseteric ridge, ventral to the anterior border of M1 (Fig. 4E).

Zygomaticomandibularis

The zygomaticomandibularis is a muscle less acknowledged in the literature and less conventional in its morphology. Several authors do not recognise the zygomaticomandibularis as a separate muscle from the deep masseter in rodents (Hiiemae & Houston, 1971; Byrd, 1981; Satoh, 1997, 1998, 1999). In contrast, we found that on micro-CT there is a clear distinction between the deep masseter and the zygomaticomandibularis in the mouse, as is also found in the squirrel, rat and guinea pig (Cox & Jeffery, 2011). A clear division between an anterior and posterior part of this muscle, as well as a rostral expansion termed the infraorbital zygomaticomandibularis are also found here in the mouse.

Viewed as a whole, the zygomaticomandibularis begins anteriorly as a small bulb-like muscle sitting in a fossa in the maxillary bone anterodorsal to the infraorbital foramen. This muscle then passes posteriorly through the infraorbital foramen, attaching along the length of the jugal bone on the mediodorsal surface. The zygomaticomandibularis then

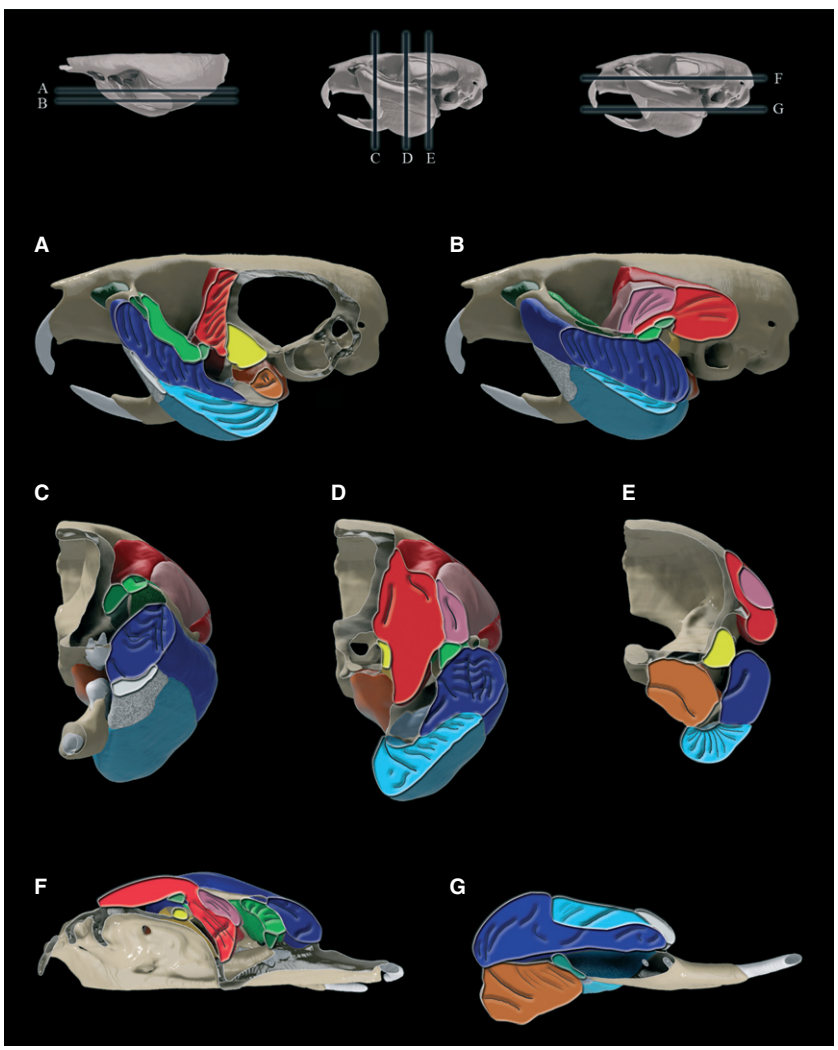

Fig. 6 Cross-sections of the three-dimensional reconstruction of *Mus musculus* craniofacial anatomy, with fibre orientations highlighted. (A) and (B) Sagittal sections moving mediolaterally; (C-E) coronal sections moving anteroposteriorly; (F,G) transverse sections moving dorsoventrally. See Fig. 3 for colour key.

travels ventrally, medial to the jugal bone, to attach onto the dorsolateral surface of the mandible (Fig. 3). Despite the length of the entire zygomaticomandibularis being greater than that of the deep masseter, this is a slim and relatively short muscle which, viewed as a whole, still accounts for only 9% of the total masticatory muscle mass in the mouse (Table 1). Below we approach and describe this muscle as its three constituent parts: the infraorbital zygomaticomandibularis, the anterior zygomaticomandibularis and the posterior zygomaticomandibularis.

Anterior zygomaticomandibularis

The anterior zygomaticomandibularis is the largest part of this muscle, accounting for 58% of its total muscle mass.

This muscle originates from the dorsomedial surface of the zygomatic arch, anteriorly from the point of greatest curvature on the medial surface of the zygomatic process of the maxilla, to the jugosquamosal suture of the jugal bone (Fig. 4B). There is also a small attachment area of this muscle on the maxillary bone, posteroventral to the zygomatic process of the maxilla (Fig. 4A). Muscles fibres run ventrally to attach onto the lateral surface of the mandible.

The anterior zygomaticomandibularis inserts onto the lateral surface of the mandible, with an attachment area that encompasses almost the entirety of the coronoid. Sitting directly dorsal to the attachment of the deep masseter, this attachment runs obliquely from a point ventral to the first molar towards the coronoid process, sparing the very tip of this coronoid where the lateral temporalis attaches. The anterior zygomaticomandibularis attachment continues posterior of the coronoid, finishing at the point of greatest curvature between the coronoid process and the condylar process, where it meets the attachment of the posterior zygomaticomandibularis (Fig. 4E).

The zygomaticomandibularis also has a thick tendinous band that inserts onto the lateral surface of the mandible, ventral to the anterior border of M1 and anterior to the attachment of the deep masseter (Figs 3 and 4E). In addition to its attachment area on the lateral surface of the coronoid, fibres from the anterior zygomaticomandibularis insert onto this tendon.

Posterior zygomaticomandibularis

Accounting for just 13% of the total mass of the zygomaticomandibularis, the posterior section is the smallest of the three parts of the zygomaticomandibularis (Table 1). This small muscle forms a bridge between the very posterior portion of the jugal bone and the mandible.

The posterior zygomaticomandibularis originates from a small area of bone on the lateral posterior border of the jugal bone, at the point where the squamosal bones extend to meet the jugosquamosal suture. This slim attachment area lies directly posterolateral to the lateral expansion of the attachment of the medial temporalis onto the squamosal bone.

Fibres of the posterior zygomaticomandibularis pass anteroventrally, lateral to the jugal bone, to insert onto the lateral surface of the mandible. Again this is a relatively small attachment area, extending from the posterior border of the attachment of the anterior zygomaticomandibularis at the point of greatest curvature between the coronoid process and the condylar process, to a point just anterior to the condylar process. This attachment area lies directly dorsal to the attachment of the deep masseter (Fig. 4E).

Infraorbital zygomaticomandibularis

The infraorbital zygomaticomandibularis is again a relatively small masticatory muscle in the mouse, accounting for 27% of the muscle mass of the zygomaticomandibularis, but only 2.4% of the overall muscle mass. This is a distinctive muscle, lying in a fossa on the maxilla anterior to the infraorbital foramen, passing posteriorly through the infraorbital foramen and then ventrally, medial to the jugal bone to attach onto the lateral surface of the mandible.

The infraorbital zygomaticomandibularis originates from a concavity in the maxilla, ventral to the nasal bone, medial to the zygomatic process of the maxilla, anterior to the orbit, and posterior to the premaxillomaxillary suture. The infraorbital zygomaticomandibularis attaches onto the lateral border of this concavity and also onto the medial surface of the zygomatic process of the maxilla (Fig. 4).

Fibres of the infraorbital zygomaticomandibularis pass posteriorly through the infraorbital foramen, and then once through the foramen, immediately descend ventrally, medial to the jugal bone, to insert onto the lateral surface of the mandible. This insertion is via a thick tendinous band that has a relatively small attachment area directly ventral to the anterior border of M1, anterior to the attachment of the deep masseter and immediately dorsal to the attachment area of the superficial masseter (Fig. 4E). Fibres of the infraorbital zygomaticomandibularis are joined by fibres of the anterior zygomaticomandibularis in their attachment to this tendinous band. Although it is difficult to determine on the micro-CT images and, due to the small size of these muscles, on dissection, fibres from the infraorbital zygomaticomandibularis may also attach to the medial border of the jugal bone or join those of the anterior zygomaticomandibularis as these two muscles run ventrally together to attach to the tendon.

Temporalis

The temporalis muscle is a major masticatory muscle, accounting for 22% of the overall muscle mass, and is thus the second largest masticatory muscle in the mouse. In rats (Cox & Jeffery, 2011) a clear division of the temporalis into lateral and medial parts is reported. A similar separation of the temporalis is reported in many rodents and other Glires,

although various terminology is used throughout the literature, and this muscle is most often described as consisting of anterior and posterior parts (Turnbull, 1970; Hiiemae & Houston, 1971; Gorniak, 1977; Woods & Howland, 1979; Druzinsky, 2010a; Druzinsky et al. 2011). A division into lateral and medial parts is apparent in the mouse; however, the exact boundaries of this division are equivocal on the micro-CT scan utilised in this study, especially as regards the superior region of the margin between the two parts. In this investigation we therefore report the temporalis muscle as medial and lateral parts but are cautious about the precise boundary and attachment points of the lateral temporalis (Fig. 3). It is estimated that the lateral temporalis is the smaller portion, accounting for 23% of the overall temporalis muscle mass, whereas the medial portion accounts for 77% (Table 1).

Medial temporalis

The medial temporalis originates from a large area on the lateral surface of the cranium. This broad attachment to the floor of the temporal fossa extends as far posteriorly as the occipitoparietal suture and as far anteriorly as the posterior boundary of the first molar. There also appears to be a lateral expansion of the attachment of the medial temporalis onto the zygomatic process of the squamosal bone. This attachment is seen to extend as far laterally as the jugosquamosal suture (Fig. 4).

Fibres of the medial temporal muscle run anteroventrally from the posterior margin of the origin until the anterior border of the attachment on the temporal fossa, where they pass ventrally down the deepest and most medial part of the frontal bone, medial to the jugal bone to insert onto the medial surface of the mandible. The attachment area of the medial temporalis is a large region directly dorsal to that of the *pars reflecta* of the superficial masseter and anterior to that of the external pterygoid. Encompassing the medial surface of the coronoid process, this insertion extends ventrally to the dental ridge and posteriorly to the point of greatest curvature between the coronoid and condyloid processes (Fig. 4F).

Lateral temporalis

It is estimated that the lateral temporalis originates from the lateral surface of the medial temporalis. The true origin of this lateral portion is likely to be an aponeurosis or fascia overlying the medial temporalis, although this is difficult to determine with any clarity on micro-CT. Micro-CT images do show a septa between the lateral and medial parts of the temporalis, and fibre orientation differs slightly between the two parts, yet a fascial layer cannot be ascertained via this methodology (Fig. 5). On dissection no comprehensive or significant fascia could be found overlying the temporalis muscle and, possibly due to the small size of the muscle, no clear division between a lateral and medial part could be found.

Fibres of the lateral temporalis run anteroventrally, passing medial to the jugal bone, alongside but lateral to the fibres of the medial temporalis. This small muscle then attaches to the tip and a small area of the lateral surface of the coronoid process (Fig. 4E).

Pterygoids

The pterygoid muscles jointly account for 16% of the overall masticatory muscle mass. Of this, 16% the external pterygoid accounts for 29% and the larger internal pterygoid for 71% (Table 1).

Fibre orientation in the pterygoids is difficult to resolve via micro-CT, but significant septa were apparent in both the internal and external muscles.

External pterygoid

The external pterygoid is a relatively small muscle compared with other masticatory muscles such as the deep masseter, accounting for just 5% of the overall muscle mass (Fig. 3).

The external pterygoid originates from the cranial base, with an attachment area that lies just anterior to the tympanic bulla, extends laterally from the palatine process to the alisphenosquamosal suture (Fig. 4C).

This small muscle then passes ventrolaterally to insert onto the medial surface of the condylar process, just ventral to the articular surface of the mandible (Fig. 4F).

Internal pterygoid

The internal pterygoid is the larger of the two pterygoid muscles, accounting for 12% of the overall masticatory muscle mass in the mouse, giving this muscle a greater mass than that of the total zygomaticomandibularis muscle.

The internal pterygoid originates from the cranial base, with an attachment area that surprisingly is approximately half the size of that of its external counterpart. This attachment area runs medially from the palatine process to the pterygoid process, lying medial to the attachment of the external pterygoid (Figs 2C and 4C).

The internal pterygoid muscle then passes posteroventrally as well as medially to insert onto the medial surface of the angle of the mandible, directly dorsal to the reflected attachment of the superficial masseter. This attachment area spans almost the entirety of the angle of the mandible as well as projecting anteriorly to almost meet the attachment of the *pars reflecta* of the superficial masseter (Fig. 4F).

Discussion

The bony anatomy of the craniofacial complex is diverse in mammals and, as follows, so is muscle architecture. The high diversity of masticatory morphology has in turn led to diversity in nomenclature. With masticatory muscles particularly unique when compared with other mammalian

groups, rodent morphology has been the focus of many investigations over the years (Cox & Jeffery, 2011; Druzinsky et al. 2011). Despite numerous studies on the masticatory anatomy of rodents in general, nomenclature and muscle division are incompatible and inconsistent between authors.

Following the terminology of Cox & Jeffery (2011), distinct muscles were determined through both dissection and detailed 3D segmentation and reconstruction of one *Mus musculus* individual with six well defined muscles identified and described.

As in all other published studies using the same methodology (Cox & Jeffery, 2011; Tsai & Holliday, 2011; Hautier et al. 2012) only one individual of the species had its craniofacial musculature reconstructed from a contrast-enhanced micro-CT scan; however, initially both left and right sides were reconstructed for intra-individual comparative purposes. This approach was coupled with classical dissection techniques to control for intraspecific variation. Although classical dissection methods are still valid and can provide highly detailed and accurate anatomical knowledge, for very small species such as the mouse this methodology can be problematic. Small yet highly significant reflections of muscles, such as the pars reflecta, which has been used previously to define the hystricognathous condition of the jaw (Woods, 1972), are almost impossible to determine with confidence or accuracy by means of dissection but are revealed using reconstruction techniques. Reconstruction of contrast-enhanced micro-CT is not only advantageous in the anatomical investigation of small species but also provides a non-destructive method where soft-tissue and muscle layers can be examined *in situ*, providing accurate information regarding their relationships with one another without the need to remove or retract superficial layers of tissue. This technique also has the advantage that greater time and consideration can be given to the segmentation of structures and if detectable errors are made, these can be re-examined and corrected as many times as required without the need to start anew. However, boundaries between closely integrated muscles, such as the lateral and medial parts of the same muscles, are not always clearly visible on these scans. In this study the boundary and precise attachment of the lateral temporalis were indistinct. Although the medial temporalis clearly originates from the bone of the temporal fossa, it is difficult to distinguish whether any fibres of the lateral temporalis have their origin in the skull, or whether lateral temporalis fibres have their origin in an aponeurosis overlying the medial temporalis. Cox & Jeffery (2011) describe the latter arrangement in both the rat and squirrel, with the origin of the lateral temporalis extending over a large surface of the medial temporalis in the rat in comparison with a much more limited origin in the squirrel. These authors also describe difficulty resolving clear medial and lateral parts to the temporalis in the guinea pig (Cox & Jeffery, 2011). Additionally, although it is possible that muscle shrinkage may occur with the iodine contrast-enhanced micro-CT technique, there is no discernible bias when comparing muscle volumes established by this technique with those measured following dissection (Table 1) and thus it may be assumed that any effect of muscle shrinkage is less than that of intraspecific variation.

Combining the results of both classical dissection and the contemporary method of contrast-enhanced micro-CT reconstruction provides a highly accurate and clear anatomical investigation of this thus-far largely undescribed region.

A unique finding of this study is the lateral expansion of the medial temporalis onto the zygomatic process of the squamosal bone in the mouse. Many previous studies regarding the masticatory musculature of rodents do not note such an attachment of the temporalis muscle onto the dorsal surface of the posterior portion of the jugal bone (Turnbull, 1970; Patel, 1978; Satoh & Iwaku, 2009; Cox & Jeffery, 2011). Satoh & Iwaku (2006) do, however, make reference to a suprazygomatic portion of the temporalis muscle in *Onychomys leucogaster*, and a number of authors describe a third division of the temporalis by distinguishing the ventral-most fibres of this muscle, often those fibres have their origin from the zygomatic process of the squamosal (Woods, 1972; Weijs, 1973; Satoh & Iwaku, 2006; Hautier & Saksiri, 2009; Druzinsky, 2010a). Hautier (2010) describes a unique arrangement of a third temporalis division in *Ctenodactylus,* although it is suggested that this is not universal among rodents but instead results from the distal position of the eye in this species, leading to a lateral displacement of the temporalis (Hautier, 2010; Cox & Jeffery, 2011).

Recently renewed attention has been given to a possible function of the temporal fascia in primates in aiding the zygomatic arch to resist the tensions of the masseter muscle exerted during biting (Eisenberg & Brodie, 1965; Curtis et al. 2011). Curtis et al. (2011) suggest that the substantial temporal fascia found in primates plays a critical role in stabilising the arch during biting. During biting, the bulge of the contracted temporalis results in a tensioned temporalis fascia which has been shown to generate a force great enough to oppose the downwards pull of the masseter (Curtis et al. 2011).

In this current study no temporal fascia of substance was found in the mouse either with dissection or segmentation. Little to no attention is given to, or observation made of, the temporalis fascia in the literature regarding the rodent masticatory apparatus (Turnbull, 1970; Patel, 1978; Satoh & Iwaku, 2006, 2009; Cox & Jeffery, 2011). We might therefore conclude that despite both the sizeable deep masseter and the anterior and posterior regions of the zygomaticomandibularis attaching onto the zygomatic arch, in the mouse, and likely also in rodents, the temporal fascia plays no role in stabilising the arch during mastication. However, the lateral expansion of the attachment of temporalis onto the posterodorsal region of the zygomatic arch extending as

far as the zygomaticosquamosal suture found in this investigation could be hypothesised to show a biomechanical solution in rodents analogous to that seen in primates, where the temporalis fascia may play an important role in stabilising the arch during downward loading. Fibre direction in this region is not consistently clear on the contrast-enhanced micro-CT; however, in regions where some direction does become apparent this appears to be consistent with a counterbalancing function. Such a discovery could prove to be a critical consideration when modelling mouse craniofacial anatomy for techniques such as FEA. Further investigation is needed to determine more precisely the nature and effect of this attachment and additionally whether such an arrangement is extended to other rodent species.

Other findings of this investigation provide an interesting comparison with other rodents and mammals. A dorsal elongation of the reflected part of the superficial masseter onto the medial surface of the mandible was identified in this investigation. This masseteric extension, termed the pars reflecta, has been reported in the rat and other rodents (Turnbull, 1970; Woods, 1972; Weijs, 1973; Hautier & Saksiri, 2009; Cox & Jeffery, 2011; Druzinsky et al. 2011). Such an extension was found to be present in both rodents and lagomorphs but not in primates, with carnivores and ungulates also possessing masseteric extensions. The latter suggests that extensions of the masseter may have evolved independently several times in mammals to aid the production of large forces at the anterior dentition (Druzinsky et al. 2011).

Perhaps the greatest implication of this current work is the potential for future applications in biomechanical modelling to further the utility of the mouse, and of other myomorph rodents including the rat in the understanding of form–function relationships in evolution and other fields. For instance, to carry out FEA, accurate data regarding muscle origin, attachment, mass, fibre orientation and general anatomy are required. In the past 10 years, FEA has been used as a modelling technique capable of answering questions in vertebrate biomechanics and evolution that could not previously be answered and thus remained largely unexplored. With the advent and availability of superb 3D imaging and robust computing power, morphologists can now address questions using engineering tools such as FEA that allow the construction of highly controlled *in silico* experiments. These techniques not only provide great benefit to the field of biomechanics in general (Chegini et al. 2009; Amin et al. 2011; Elkins et al. 2011) but are also playing an ever-increasing and central role in craniofacial biomechanics, allowing detailed and precise descriptions and comparisons of mechanical performance in different species and morphologies (Koolstra et al. 1988; Moazen et al. 2008; Moreno et al. 2008; Tseng, 2009; Chalk et al. 2011; Gröning et al. 2011a, b; Nakashige et al. 2011; Panagiotopoulou et al. 2011; Reed et al. 2011).

Computational simulations require a vast array of accurate data to produce biologically meaningful models of the craniofacial skeleton. Such necessary data includes the precise anatomical description relevant craniofacial tissues, data concerning the material properties of these tissues, and information regarding feeding mechanics that may be established through *in vivo* electromyography and kinematics (Gorniak, 1977; Cobb, 2011). Although traditionally, knowledge of feeding patterns and mechanics was gained through electromyographical work, the accessibility of such techniques as well as ethical considerations has meant that there is a paucity of such important data. Where electromyography is not available or suitable, MDA is now a possible technique for the prediction of muscle activation patterns (Koolstra & van Eijden, 1992; Iwasaki et al. 2003; Westneat, 2003; Alfaro et al. 2004; Westneat, 2004; Grubich & Westneat, 2006; de Zee et al. 2007; Curtis et al. 2008, 2010a, 2010b, 2011; Moazen et al. 2008, 2009a,b; Bates & Falkingham, 2012) Still a relatively uncommon method in mammalian taxa, MDA may be used to model the movements and forces between structures such as the cranium and mandible and in turn allows the prediction of muscle activation during feeding, modelling of jaw motion, and the investigation of the function of muscle parameters such as fibre length and muscle tension (Langenbach & Hannam, 1999; Peck et al. 2000; Hannam et al. 2008). As with FEA, MDA requires as a prerequisite detailed and accurate anatomical descriptions of the relevant craniofacial tissues such as the muscles of mastication, and it is this description which this study provides for the mouse.

This study forms a preliminary basis for a series of future experimental applications. In prospective studies, mouse models will be used to address questions regarding modularity, integration and plasticity in the craniofacial complex. These and other concepts key to our understanding of evolution may be elegantly explored through the use of the mouse as a model organism, with the use of knockout mice allowing valuable experimental models to be created. The detailed and precise anatomical knowledge acquired in the current study permits the precise construction of biologically accurate representations of relevant anatomy and as such allows questions of biological and functional significance to be addressed accurately.

Acknowledgements

The authors thank both Laura Fitton and Philip Cox in the Centre for Anatomical and Human Sciences, HYMS, for their help, comments and support.

References

Alfaro ME, Bolnick DI, Wainwright PC (2004) Evolutionary dynamics of complex biomechanical systems: an example using the four-bar mechanism. *Evolution* **58**, 495–503.

Amin S, Kopperdhal DL, Melton LJ, et al. (2011) Association of hip strength estimates by finite-element analysis with fractures in women and men. *J Bone Miner Res* **26**, 1593–1600.

Aslanidi O, Nikolaidou T, Zhao J, et al. (2012) Application of micro-computed tomography with iodine staining to cardiac imaging, segmentation and computational model development. *IEEE Trans Med Imaging* **32**, 8–17.

Atchley WR, Plummer AA, Riska B (1985a) Genetic analysis of size-scaling patterns in the mouse mandible. *Genetics* **111**, 579–595.

Atchley WR, Plummer AA, Riska B (1985b) Genetics of mandible form in the mouse. *Genetics* **111**, 555–577.

Atchley WR, Newman S, Cowley DE (1988) Genetic divergence in mandible form in relation to molecular divergence in inbred mouse strains. *Genetics* **120**, 239–253.

Auffray JC, Alibert P, Latieule C, et al. (1996) Relative warp analysis of skull shape across the hybrid zone of the house mouse (*Mus musculus*) in Denmark. *J Zool* **240**, 441–455.

Badea CT, Drangova M, Holdsworth DW, et al. (2008) In vivo small-animal imaging using micro-CT and digital subtraction angiography. *Phys Med Biol* **53**, R319.

Ball SS, Roth VL (1995) Jaw muscles of new-world squrrels. *J Morphol* **22**, 4.

Bates KT, Falkingham PL (2012) Estimating maximum bite performance in *Tyrannosaurus rex* using multi-body dynamics. *Biol Lett* **8**, 660–664.

Berry RJA (1900) The true cæcal apex, or the vermiform appendix: its minute and comparative anatomy. *J Anat Physiol* **35**, 83–100.

Boughner JC, Wat S, Diewert VM, et al. (2008) Short-faced mice and developmental interactions between the brain and the face. *J Anat* **213**, 646–662.

Brune RM, Bard JBL, Dubreuil C, et al. (1999) A three-dimensional model of the mouse at embryonic day 9. *Dev Biol* **216**, 457–468.

Byrd KE (1981) Mandibular movement and muscle activity during mastication in the guinea pig (*Cavia porcellus*). *J Morphol* **170**, 147–169.

Byron CD, Borke J, Yu J, et al. (2004) Effects of increased muscle mass on mouse sagittal suture morphology and mechanics. *Anat Rec A Discov Mol Cell Evol Biol* **279A**, 676–684.

Byron CD, Maness H, Yu JC, et al. (2008) Enlargement of the temporalis muscle and alterations in the lateral cranial vault. *Integr Comp Biol* **48**, 338–344.

Chai Y, Maxson RE (2006) Recent advances in craniofacial morphogenesis. *Dev Dyn* **235**, 2353–2375.

Chalk J, Richmond BG, Ross CF, et al. (2011) A finite element analysis of masticatory stress hypotheses. *Am J Phys Anthropol* **145**, 1–10.

Chegini S, Beck M, Ferguson SJ (2009) The effects of impingement and dysplasia on stress distributions in the hip joint during sitting and walking: a finite element analysis. *J Orthop Res* **27**, 195–201.

Cheverud JM, Hartmann D, Richtsmeier JT, et al. (1991) A quantitative genetic analysis of localized morphology in mandibles of inbred mice using finite element scaling analysis. *J Craniofac Genet Dev Biol* **11**, 122–137.

Christian Peter K (2002) Morphometrics and the role of the phenotype in studies of the evolution of developmental mechanisms. *Gene* **287**, 3–10.

Cobb SN (2011) Craniofacial biomechanics: in vivo to in silico. *J Anat* **218**, 1–2.

Coldiron RW (1977) On the jaw musculature and relationships of *Petrodomus tetradactylus* (Mammalia, Macroscelidea). *Am Mus Novit* **2613**, 1–12.

Cordeiro-Estrela P, Baylac M, Denys C, et al. (2006) Interspecific patterns of skull variation between sympatric Brazilian vesper mice: geometric morphometrics assessment. *J Mammal* **87**, 1270–1279.

Corti M, Rohlf FJ (2001) Chromosomal speciation and phenotypic evolution in the house mouse. *Biol J Linn Soc* **73**, 99–112.

Cox PG, Jeffery N (2011) Reviewing the morphology of the jaw-closing musculature in squirrels, rats, and guinea pigs with contrast-enhanced microCT. *Anat Rec* **294**, 915–928.

Cox PG, Rayfield EJ, Fagan MJ, et al. (2012) Functional evolution of the feeding system in rodents. *PLoS ONE* **7**, e36299.

Cray J, Kneib J, Vecchione L, et al. (2011) Masticatory hypermuscularity is not related to reduced cranial volume in myostatin-knockout mice. *Anat Rec* **294**, 1170–1177.

Curtis N (2011) Craniofacial biomechanics: an overview of recent multibody modelling studies. *J Anat* **218**, 16–25.

Curtis N, Kupczik K, O'Higgins P, et al. (2008) Predicting skull loading: applying multibody dynamics analysis to a macaque skull. *Anat Rec* **291**, 491–501.

Curtis N, Jones MEH, Evans SE, et al. (2010a) Predicting muscle activation patterns from motion and anatomy: modelling the skull of Sphenodon (Diapsida: Rhynchocephalia). *J R Soc Interface* **7**, 153–160.

Curtis N, Jones MEH, Lappin AK, et al. (2010b) Comparison between in vivo and theoretical bite performance: using multi-body modelling to predict muscle and bite forces in a reptile skull. *J Biomech* **43**, 2804–2809.

Curtis N, Witzel U, Fitton L, et al. (2011) The mechanical significance of the temporal fasciae in *Macaca fascicularis*: an investigation using finite element analysis. *Anat Rec* **294**, 1178–1190.

Debat V, Milton CC, Rutherford S, et al. (2006) *Evolution* **60**, 2529.

Druzinsky RE (2010a) Functional anatomy of incisor biting in *Aplodontia rufa* and sciuromorph rodents – part 1: masticatory muscles, skull shape and digging. *Cells Tissues Organs* **191**, 510–522.

Druzinsky RE (2010b) Functional anatomy of incisor biting in *Aplodontia rufa* and sciuromorph rodents – part 2: sciuromorphy is efficacious for production of force at the incisors. *Cells Tissues Organs* **192**, 50–62.

Druzinsky RE, Doherty AH, De Vree FL (2011) Mammalian masticatory muscles: homology, nomenclature, and diversification. *Integr Comp Biol* **51**, 224–234.

Eisenberg NA, Brodie AG (1965) Antagonism of temporal fascia to masseteric contraction. *Anat Rec* **152**, 185–192.

Elkins JM, Stroud NJ, Rudert MJ, et al. (2011) The capsule's contribution to total hip construct stability – a finite element analysis. *J Orthop Res* **29**, 1642–1648.

Freeman PW, Lemen CA (2008a) Measuring bite force in small mammals with a piezo-resistive sensor. *J Mammal* **89**, 513–517.

Freeman PW, Lemen CA (2008b) A simple morphological predictor of bite force in rodents. *J Zool* **275**, 418–422.

Gorniak GC (1977) Feeding in golden hamsters, *Mesocricetus auratus*. *J Morphol* **154**, 427–458.

Greene EC (1936) Anatomy of the rat. *Am J Med Sci* **191**, 858.

Gröning F, Fagan MJ, O'Higgins P (2011a) The effects of the periodontal ligament on mandibular stiffness: a study combining

finite element analysis and geometric morphometrics. *J Biomech* **44**, 1304–1312.

Gröning F, Liu J, Fagan MJ, et al. (2011b) Why do humans have chins? Testing the mechanical significance of modern human symphyseal morphology with finite element analysis. *Am J Phys Anthropol* **144**, 593–606.

Grubich JR, Westneat MW (2006) Four-bar linkage modelling in teleost pharyngeal jaws: computer simulations of bite kinetics. *J Anat* **209**, 79–92.

Hallgrimsson B, Lieberman DE (2008) Mouse models and the evolutionary developmental biology of the skull. *Integr Comp Biol* **48**, 373–384.

Hallgrímsson B, Dorval CJ, Zelditch ML, et al. (2004a) Craniofacial variability and morphological integration in mice susceptible to cleft lip and palate. *J Anat* **205**, 501–517.

Hallgrímsson B, Willmore K, Dorval C, et al. (2004b) Craniofacial variability and modularity in macaques and mice. *J Exp Zool B Mol Dev Evol* **302B**, 207–225.

Hallgrímsson B, Brown JJY, Ford-Hutchinson AF, et al. (2006) The brachymorph mouse and the developmental-genetic basis for canalization and morphological integration. *Evol Dev* **8**, 61–73.

Hallgrímsson B, Lieberman DE, Liu W, et al. (2007) Epigenetic interactions and the structure of phenotypic variation in the cranium. *Evol Dev* **9**, 76–91.

Hannam AG, Stavness I, Lloyd JE, et al. (2008) A dynamic model of jaw and hyoid biomechanics during chewing. *J Biomech* **41**, 1069–1076.

Hautier L (2010) Masticatory muscle architecture in the gundi *Ctenodactylus vali* (Mammalia, Rodentia). *Mammalia* **74**, 153.

Hautier L, Saksiri S (2009) Masticatory muscle architecture in the Laotian rock rat *Laonastes aenigmamus* (Mammalia, Rodentia): new insights into the evolution of hystricognathy. *J Anat* **215**, 401–410.

Hautier L, Lebrun R, Cox PG (2012) Patterns of covariation in the masticatory apparatus of hystricognathous rodents: implications for evolution and diversification. *J Morphol* **273**, 1319–1337.

Hiiemäe KM, Ardran GM (1968) A cinefluorographic study of mandibular movement during feeding in the rat (*Rattus norvegicus*). *J Zool* **154**, 139–154.

Hiiemae K, Houston WJB (1971) The structure and function of the jaw muscles in the rat (*Rattus norvegicus* L.). *Zool J Linn Soc* **50**, 75–99.

Hill CA, Reeves RH, Richtsmeier JT (2007) Effects of aneuploidy on skull growth in a mouse model of Down syndrome. *J Anat* **210**, 394–405.

Iwasaki LR, Petsche PE, McCall WD Jr, et al. (2003) Neuromuscular objectives of the human masticatory apparatus during static biting. *Arch Oral Biol* **48**, 767–777.

Janis CM (1983) Muscles of the masticatory apparatus in two genera of hyraces (*Procavia* and *Heterohyrax*). *J Morphol* **176**, 61–87.

Jeffery N, Stephenson R, Gallagher JA, et al. (2011) Microcomputed tomography with iodine staining resolves the arrangement of muscle fibres. *J Biomech* **44**, 189–192.

Kaufman MH (1992) *The Atlas of Mouse Development*. London: Academic Press.

Kaufman MH, Bard JBL (1999) *The Anatomical Basis of Mouse Development*. San Diego: Academic Press.

Kawakami M, Yamamura K-I (2008) Cranial bone morphometric study among mouse strains. *BMC Evol Biol* **8**, 73.

Klingenberg CP, Leamy LJ (2001) Quantitative genetics of geometric shape in the mouse mandible. *Evolution* **55**, 2342–2352.

Klingenberg CP, Mebus K, Auffray J-C (2003) Developmental integration in a complex morphological structure: how distinct are the modules in the mouse mandible? *Evol Dev* **5**, 522–531.

Klintworth GK (1968) The comparative anatomy and phylogeny of the tentorium cerebelli. *Anat Rec* **160**, 635–641.

Koolstra JH, van Eijden TMGJ (1992) Application and validation of a three-dimensional mathematical model of the human masticatory system in vivo. *J Biomech* **25**, 175–187.

Koolstra JH, van Eijden TMGJ, Weijs WA, et al. (1988) A three-dimensional mathematical model of the human masticatory system predicting maximum possible bite forces. *J Biomech* **21**, 563–576.

Kyrkanides S, Kambylafkas P, Miller JH, et al. (2007) The cranial base in craniofacial development: a gene therapy study. *J Dent Res* **86**, 956–961.

Langenbach GEJ, Hannam AG (1999) The role of passive muscle tensions in a three-dimensional dynamic model of the human jaw. *Arch Oral Biol* **44**, 557–573.

Leamy L (1993) Morphological integration of fluctuating asymmetry in the mouse mandible. *Genetica* **89**, 139–153.

Lieberman DE, Hallgrímsson B, Liu W, et al. (2008) Spatial packing, cranial base angulation, and craniofacial shape variation in the mammalian skull: testing a new model using mice. *J Anat* **212**, 720–735.

Lozanoff S, Jureczek S, Feng T, et al. (1994) Anterior cranial base morphology in mice with midfacial retrusion. *Cleft Palate Craniofac J* **31**, 417–428.

Macholán M (2008) The mouse skull as a source of morphometric data for phylogeny inference. *Zool Anz* **247**, 315–327.

Macholán M, Mikula O, Vohralík V (2008) Geographic phenetic variation of two eastern-Mediterranean non-commensal mouse species, *Mus macedonicus* and *M. cypriacus* (Rodentia: Muridae) based on traditional and geometric approaches to morphometrics. *Zool Anz* **247**, 67–80.

Maedaa N, Kawasaki T, Osawa K, et al. (1987) Effects of long-term intake of a fine-grained diet on the mouse masseter muscle. *Acta Anat (Basel)* **128**, 326–333.

Metscher B (2009) MicroCT for comparative morphology: simple staining methods allow high-contrast 3D imaging of diverse non-mineralized animal tissues. *BMC Physiology* **9**, 11.

Mezey JG, Cheverud JM, Wagner GP (2000) Is the genotype–phenotype map modular?: a statistical approach using mouse quantitative trait loci data. *Genetics* **156**, 305–311.

Moazen M, Curtis N, Evans SE, et al. (2008) Combined finite element and multibody dynamics analysis of biting in a *Uromastyx hardwickii* lizard skull. *J Anat* **213**, 499–508.

Moazen M, Curtis N, O'Higgins P, et al. (2009a) Biomechanical assessment of evolutionary changes in the lepidosaurian skull. *Proc Natl Acad Sci U S A* **106**, 8273–8277.

Moazen M, Curtis N, O'Higgins P, et al. (2009b) Assessment of the role of sutures in a lizard skull: a computer modelling study. *Proc R Soc Lond B Biol Sci* **276**, 39–46.

Moreno K, Wroe S, Clausen P, et al. (2008) Cranial performance in the Komodo dragon (*Varanus komodoensis*) as revealed by high-resolution 3-D finite element analysis. *J Anat* **212**, 736–746.

Morriss-Kay GM, Wilkie AOM (2005) Growth of the normal skull vault and its alteration in craniosynostosis: insights from human genetics and experimental studies. *J Anat* **207**, 637–653.

Mosley JR, Lanyon LE (1998) Strain rate as a controlling influence on adaptive modeling in response to dynamic loading of the ulna in growing male rats. *Bone* **23**, 313–318.

Murphy RA, Beardsly AC (1974) Mechanical properties of the cat soleus muscle in situ. *Am J Physiol* **227**, 1008–1013.

Nakashige M, Smith AL, Strait DS (2011) Biomechanics of the macaque postorbital septum investigated using finite element analysis: implications for anthropoid evolution. *J Anat* **218**, 142–150.

Nies M, Young Ro J (2004) Bite force measurement in awake rats. *Brain Res Protoc* **12**, 180–185.

Offermans M, De Vree F (1989) Morphology of the masticatory apparatus in the springhare, *Pedetes capensis*. *J Mammal* **70**, 701–711.

Olivares AI, Verzi DH, Vassallo AI (2004) Masticatory morphological diversity and chewing modes in South American caviomorph rodents (family Octodontidae). *J Zool* **263**, 167–177.

Panagiotopoulou O, Kupczik K, Cobb SN (2011) The mechanical function of the periodontal ligament in the macaque mandible: a validation and sensitivity study using finite element analysis. *J Anat* **218**, 75–86.

Parsons TE, Kristensen E, Hornung L, et al. (2008) Phenotypic variability and craniofacial dysmorphology: increased shape variance in a mouse model for cleft lip. *J Anat* **212**, 135–143.

Patel NG (1978) Functional morphology of the masticatory muscles of *Mus musculus*. *Proc Indian Acad Sci* **5**, 1–57.

Peck CC, Langenbach GEJ, Hannam AG (2000) Dynamic simulation of muscle and articular properties during human wide jaw opening. *Arch Oral Biol* **45**, 963–982.

Perlyn CA, DeLeon VB, Babbs C, et al. (2006) The craniofacial phenotype of the crouzon mouse: analysis of a model for syndromic craniosynostosis using three-dimensional MicroCT. *Cleft Palate Craniofac J* **43**, 740–748.

Pomikal C, Streicher J (2010) 4D-analysis of early pelvic girdle development in the mouse (*Mus musculus*). *J Morphol* **271**, 116–126.

Ravosa MJ, López EK, Menegaz RA, et al. (2008) Using 'Mighty Mouse' to understand masticatory plasticity: myostatin-deficient mice and musculoskeletal function. *Integr Comp Biol* **48**, 345–359.

Reed DA, Porro LB, Iriarte-Diaz J, et al. (2011) The impact of bone and suture material properties on mandibular function in *Alligator mississippiensis*: testing theoretical phenotypes with finite element analysis. *J Anat* **218**, 59–74.

Renaud S, Michaux JR (2007) Mandibles and molars of the wood mouse, *Apodemus sylvaticus* (L.): integrated latitudinal pattern and mosaic insular evolution. *J Biogeogr* **34**, 339–355.

Renaud S, Auffray J, de la Porte S (2010) Epigenetic effects on the mouse mandible: common features and discrepancies in remodeling due to muscular dystrophy and response to food consistency. *BMC Evol Biol* **10**, 1471–2148.

Richtsmeier JT, Zumwalt A, Carlson EJ, et al. (2002) Craniofacial phenotypes in segmentally trisomic mouse models for Down syndrome. *Am J Med Genet* **107**, 317–324.

Rinker GC (1954) The comparative myology of the mammalian genera *Sigmodon, Oryzomys, Neotoma, and Peromyscus* (Cricetinae), with remarks on their intergeneric relationships. *Misc Publ Mus Zool Univ Mich* **83**, 1–124.

Rinker GC, Hooper ET (1950) Notes on the cranial musculature in two subgenera of *Reithrodontomys* (harvest mice). *Occas Pap Mus Zool Univ Michigan* **528**, 1–11.

Roberts LH (1975) The functional anatomy of the rodent larynx in relation to audible and ultrasonic cry production. *Zool J Linn Soc* **56**, 255–264.

Robins MW (1977) Biting loads generated by the laboratory rat. *Arch Oral Biol* **22**, 43–47.

Satoh K (1997) Comparative functional morphology of mandibular forward movement during mastication of two murid rodents, *Apodemus speciosus* (Murinae) and *Clethrionomys rufocanus* (Arvicolinae). *J Morphol* **231**, 131–142.

Satoh K (1998) Balancing function of the masticatory muscles during incisal biting in two murid rodents, *Apodemus speciosus* and *Clethrionomys rufocanus*. *J Morphol* **236**, 49–56.

Satoh K (1999) Mechanical advantage of area of origin for the external pterygoid muscle in two murid rodents, *Apodemus speciosus* and *Clethrionomys rufocanus*. *J Morphol* **240**, 1–14.

Satoh K, Iwaku F (2004) Internal architecture, origin-insertion, and mass of jaw muscles in Old World hamsters. *J Morphol* **260**, 101–116.

Satoh K, Iwaku F (2006) Jaw muscle functional anatomy in northern grasshopper mouse, *Onychomys leucogaster,* a carnivorous murid. *J Morphol* **267**, 987–999.

Satoh K, Iwaku F (2009) Structure and direction of jaw adductor muscles as herbivorous adaptations in *Neotoma mexicana* (Muridae, Rodentia). *Zoomorphology* **128**, 339–348.

Storch G (1968) Funktionsmorphologische Untersuchungen an der Kaumuskulatur und an korrelierten Schaedelstrukturen der Chiropteren. *Abh Senckenb Naturforsch Ges* **517**, 1–92.

Tobin JL, Di Franco M, Eichers E, et al. (2008) Inhibition of neural crest migration underlies craniofacial dysmorphology and Hirschsprung's disease in Bardet-Biedl syndrome. *Proc Natl Acad Sci USA* **105**, 6714–6719.

Tsai HP, Holliday CM (2011) Ontogeny of the alligator cartilago transiliens and its significance for sauropsid jaw muscle evolution. *PLoS ONE* **6**, e24935.

Tseng ZJ (2009) Cranial function in a late Miocene Dinocrocuta gigantea (Mammalia: Carnivora) revealed by comparative finite element analysis. *Biol J Linn Soc* **96**, 51–67.

Turnbull WD (1970) Mammalian Masticatory Apparatus. *Fieldiana: Geology* **18**, 149–356.

Vecchione L, Byron C, Cooper GM, et al. (2007) Craniofacial morphology in myostatin-deficient mice. *J Dent Res* **86**, 1068–1072.

Weijs WA (1973) Morphology of the muscles of mastication in the Albino Rat, *Rattus norvegicus* (Berkenhout, 1769). *Acta Morphol Neerl Scand* **11**, 321–340.

Weijs WA, Dantuma R (1975) Electromyography and mechanics of mastication in the albino rat. *J Morphol* **146**, 1–33.

Westneat MW (2003) A biomechanical model for analysis of muscle force, power output and lower jaw motion in fishes. *J Theor Biol* **223**, 269–281.

Westneat MW (2004) Evolution of levers and linkages in the feeding mechanisms of fishes. *Integr Comp Biol* **44**, 378–389.

Williams SH, Peiffer E, Ford S (2009) Gape and bite force in the rodents *Onychomys leucogaster* and *Peromyscus maniculatus:* does jaw-muscle anatomy predict performance? *J Morphol* **270**, 1338–1347.

Willmore KE, Leamy L, Hallgrímsson B (2006a) Effects of developmental and functional interactions on mouse cranial variability through late ontogeny. *Evol Dev* **8**, 550–567.

Willmore KE, Zelditch ML, Young N, et al. (2006b) Canalization and developmental stability in the Brachyrrhine mouse. *J Anat* **208**, 361–372.

Wirkner CS, Prendini L (2007) Comparative morphology of the hemolymph vascular system in scorpions – a survey using corrosion casting, MicroCT, and 3D-reconstruction. *J Morphol* **268**, 401–413.

Wirkner CS, Richter S (2004) Improvement of microanatomical research by combining corrosion casts with MicroCT and 3D reconstruction, exemplified in the circulatory organs of the woodlouse. *Microsc Res Tech* **64**, 250–254.

Wood AE (1965) Grades and clades among rodents. *Evolution* **19**, 115–130.

Woods CA (1972) Comparative myology of jaw, hyoid, and pectoral appendicular regions of New and Old World hystricomorph rodents. *Bull Am Mus Nat Hist* **147**, 115–198.

Woods CA, Hermanson JW (1985) Myology of hystricognath rodents: an analysis of form, function, and phylogeny. In: *Evolutionary Relationships among Rodents*. (eds Luckett EWO, Hartenberger JL), pp. 515–548. New York: Plenum Press.

Woods CA, Howland EB (1979) Adaptive radiation of capromyid rodents: anatomy of the masticatory apparatus. *J Mammal* **60**, 95–116.

Yamada M, Koga Y, Okayasu I, et al. (2006) Influence of soft diet feeding on development of masticatory function. *J Jpn Soc Stomatognath Funct* **12**, 118–125.

Yoshikawa T, Suzuki T (1969) The comparative anatomical study of the masseter of the mammal (3). *Anat Anz* **125**, 363–387.

de Zee M, Dalstra M, Cattaneo PM, et al. (2007) Validation of a musculo-skeletal model of the mandible and its application to mandibular distraction osteogenesis. *J Biomech* **40**, 1192–1201.